COUPLED CLUSTER STUDY OF POLYCYCLOPENTANES: STRUCTURE AND PROPERTIES OF C_5H_{2n}, n = 0–4

Libor VEIS[a1], Petr ČÁRSKY[a2], Jiří PITTNER[a3] and Josef MICHL[a,b,*]

[a] *J. Heyrovský Institute of Physical Chemistry, Academy of Sciences of the Czech Republic, v. v. i., Dolejškova 3, 182 23 Prague 8, Czech Republic; e-mail:* [1] *libor.veis@jh-inst.cas.cz,* [2] *carsky@jh-inst.cas.cz,* [3] *jiri.pittner@jh-inst.cas.cz*

[b] *Department of Chemistry and Biochemistry, University of Colorado, Boulder, Colorado 80309-0215, U.S.A.; e-mail: michl@eefus.colorado.edu*

Recieved August 18, 2008
Accepted August 26, 2008
Published online December 5, 2008

Dedicated to Professor Rudolf Zahradník on the occasion of his 80th birthday.

The title hydrocarbons have been examined by the CCSD(T)/cc-pVTZ (singlets) and UMP2/cc-pVTZ (triplets) methods. They were confirmed to represent local minima on the singlet potential energy surface, while 1,3-biradical, 1,4-biradical, or carbene structures were found on the triplet surface, including an intermediate for the triplet energy transfer from one to the other double bond of 1,4-pentadiene. Bonding is discussed in terms of Weinhold's NBO theory and the absence of a simple correlation between bond strength and bond length in these highly strained systems is pointed out. Predictions of NMR, IR, and Raman spectra are provided.

Keywords: *Ab initio* calculations; Polycyclopentanes; Single-reference and multireference coupled clusters; NBO analysis; Predicted NMR spectra; Predicted IR and Raman spectra.

This study deals with bicyclo[1.1.1]pentane (**1**) and a set of fused cyclopropanes shown in Scheme 1, derived by successive replacement of pairs of hydrogen atoms with additional C–C single bonds: **2** ([1.1.1]propellane), **3** (tricyclo[2.1.0.$0^{2,5}$]pentane), **4** (tetracyclo[2.1.0.$0^{2,4}$.$0^{2,5}$]pentane), **5** (pyramidane), **6** (pentacyclo[2.1.0.$0^{1,3}$.$0^{2,5}$.$0^{3,5}$]pentane), and the carbon cluster **7** (hexacyclo[2.1.0.$0^{1,3}$.$0^{2,4}$.$0^{2,5}$.$0^{3,5}$]pentane).

Highly strained small-ring compounds have fascinated chemists for a long time. Prior to the first synthesis of cyclopropane[1] it was not at all clear that it would be stable, and nearly a hundred years later, few chemists expected [1.1.1]propellane (**2**)[2] to be isolable. Other currently improbable looking structures may turn out to have significant stability, too.

Collect. Czech. Chem. Commun. 2008, Vol. 73, No. 11, pp. 1525–1551

doi:10.1135/cccc20081525

All seven compounds **1**–**7** have attracted much attention[2–19], but only **1** [3], **2** [2], and **3** [4] have been prepared. An initial attempt to compare the members of this group of seven structures was performed at a level of theory that is considered low nowadays (MP2/6-31G*), and is easy to criticize for having ignored the potentially multireference nature of some of the ground states. We have now re-evaluated the whole series **1**–**7** at the uniform level of the more reliable coupled cluster theory, and for comparison obtained some results for the more stable linear carbon cluster C_5 (**7a**) as well.

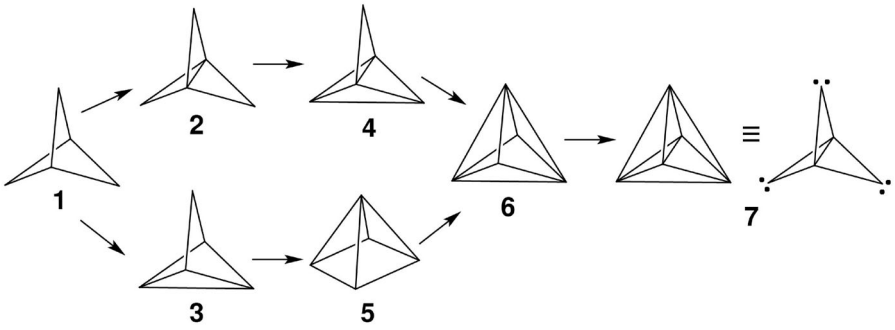

SCHEME 1
Compounds **1**–**7**

Perhaps surprisingly, the main result has survived intact: all of these hydrocarbon skeletons represent minima on the potential energy surface. Like **1**–**3**, **4**–**7** are thus expected to be stable to unimolecular rearrangements. Whether this means stability under the low-temperature conditions of argon matrix isolation or stability at room temperature cannot yet be stated, but the present results represent a starting point for the evaluation of barriers to unimolecular transformations. Previously, a high activation energy was calculated by multireference methods[15,16] for the Woodward–Hoffman forbidden disrotatory isomerization of **3** to 1,3-cyclopentadiene (**8**) through a biradicaloid transition state (Scheme 2), in agreement with its room-temperature stability. We have now recalculated the transition structure. A similar high value of activation energy has been measured and calculated for unimolecular rearragement of **2** [11], which is also unimolecularly stable at room temperature. Prior calculations suggest that unimolecular stability should be considerable even for **5**, predicted to have quite interesting and unusual properties[9,10,12].

We have also computed the lowest triplet energies of **1**–**7**, which provide an additional measure of the stability of these unusual hydrocarbons.

Intermolecular processes such as dimerization are a matter that requires future consideration, as they may prevent the isolation of **4**–**7** in bulk.

In addition to calculating ground state energies and geometries, we have computed spectroscopic properties that are likely to be important for the initial characterization of **4**–**7** if they are made in the laboratory. With a few remarkable exceptions, the computed NMR and vibrational spectra of the known hydrocarbons **1**–**3** agree very well with those observed.

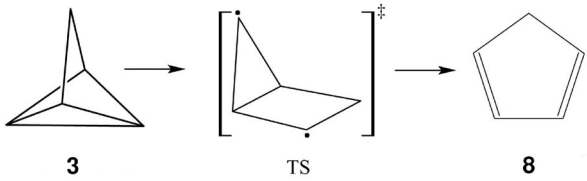

SCHEME 2
Thermal isomerization of tricyclo[2.1.0.0^{2,5}]pentane (**3**) to 1,3-cyclopentadiene (**8**) through a biradical transition state (TS)

COMPUTATIONAL METHODS

All calculations were performed with the cc-pVTZ basis set[20], except for those of indirect spin-spin coupling constants, which used the IGLO-III basis set[21] (sometimes also denoted as HIII [22]). This basis is specifically designed for calculations of NMR spin-spin coupling constants[23], as it includes a larger number of tight functions (particularly of s symmetry) than standard basis sets. It is more flexible in the neighborhood of the nucleus, which is important for the correct description of spin-spin coupling constants[22].

A CCSD(T) geometry optimization for **1**–**7** was followed by a CCSD(T) harmonic frequency calculation to confirm the optimized structures as true minima. CASSCF calculations were then performed at the optimized geometries to check whether a correct description of the electronic structure requires the use of a multireference method. Significant multireference character was found for **2**, **4** and **7**, using CAS(6,5), CAS(4,4) and CAS(8,8) active spaces, respectively. The CI coefficients of the second most important configuration, obtained from the dominant ground configuration by a double excitation from the highest occupied (HOMO) to the lowest unoccupied (LUMO) molecular orbital, were 0.19, 0.24 and 0.32, respectively. For these three structures single-point energy calculations were then performed at the CCSD(T) geometries with the recently developed and

implemented multireference Brillouin–Wigner coupled cluster method MR BWCCSD(T)[24], using the two most important configurations as reference. Energies were corrected with the *a posteriori* size-extensivity correction[25] in all multireference Brillouin–Wigner coupled cluster calculations in this report.

Heats of formation at 0 and 298 K were obtained from the calculated energies, harmonic frequencies and experimental heats of formation of atoms taken from the literature[26]. MR BWCCSD(T) heats of formation were calculated from MR BWCCSD(T) energies but with CCSD(T) harmonic frequencies, because only single point calculations were performed with the multireference method. Bonding in **1**–**7** was examined using the natural bond orbital (NBO) analysis of the CCSD electron density at the CCSD(T) optimized geometry. IR [CCSD(T)] and Raman (MP2) intensities were also calculated.

CCSD(T) GIAO NMR chemical shielding values were calculated at the optimized geometries. Methane was used as a reference compound for conversion of NMR chemical shielding values to chemical shifts. The measured chemical shifts of methane (0.23 ppm [27] for ^{1}H NMR, –2.3 ppm [28] for ^{13}C NMR) were used to convert the results to the usual tetramethylsilane (TMS) reference.

Indirect NMR spin-spin coupling constants were calculated as unrelaxed second derivatives of the CCSD energy using the unrestricted Hartree–Fock (UHF) reference. The CCSD(T) method is not recommended[29] for the calculation of indirect spin-spin coupling constants as it requires proper inclusion of orbital relaxation. The coupling constants contain four contributions: the Fermi contact term (FC), which usually dominates, the spin-dipole term (SD), and the paramagnetic (PSO) and the diamagnetic (DSO) spin-orbit terms.

Vertical excitation energies to the lowest triplet state were calculated at the CCSD(T) level of theory, using the restricted open-shell Hartree-Fock (ROHF) reference, at the CCSD(T) optimized geometries of the ground singlet states. The triplet geometries were then optimized using the UMP2(FC) (FC denotes frozen core) method and used to calculate the adiabatic excitation energies to the lowest triplet state.

The thermal isomerization of **3** to **8** was examined using a combination of single-reference and multireference methods. The geometries of **3** and **8** were optimized using the single-reference CCSD and CCSD(T) methods, and the geometry of the transition structure (TS) by the CASPT2(4,4) method. These methods were also used for the harmonic vibrational analysis of **3**, **8**, and TS. The TS exhibited a single imaginary frequency. The

search for TS started from an initial guess obtained at the CASSCF(8,8) level, which was also used to follow the intrinsic reaction coordinate in both directions to verify the connection between the reactant and product. The energies at the optimized geometries were obtained at the multireference MR BWCCSD [30–32] and MR BWCCSD(T) levels for **3**, **8**, and TS. In the case of **3**, the same result was obtained at the single-reference CC level because the ground state wave function of this structure does not exhibit a multireference character. The multireference calculations used the active space defined by the HOMO and LUMO.

The enthalpies of **3**, **8**, and TS were obtained from their potential energies, zero-point energies (ZPEs), and thermal corrections, and were used to evaluate reaction and activation enthalpies. The vertical singlet-triplet separation at the TS geometry was obtained by means of the CASPT2(4,4), MR BWCCSD, and MR BWCCSD(T) methods.

All CCSD(T) calculations were carried out using the Aces II program[33]. The NMR chemical shielding calculations were performed with the Austin–Mainz–Budapest version[29] of this program and the multireference Brillouin–Wigner coupled cluster calculations were done with a version of this program developed in our laboratory. The CCSD calculations of indirect spin-spin coupling constants were also performed with the Austin–Mainz–Budapest version of the Aces II program. The CASSCF and CASPT2 calculations were carried out using the MOLPRO program[34–36] and the calculations of Raman intensities and UMP2(FC) triplet optimizations were performed with the Gaussian 03 program[37]. NBO analysis was performed with the NBO 3.1 [38] program connected to Gaussian 03.

RESULTS

Figure 1 shows the CCSD(T) optimized geometries of **1**–**7** and Table I compares them with those obtained in previous SCF, MP2 and DFT calculations[6,19] and with those available from experiments. It also gives their total energies and provides results for the linear carbon cluster C_5 (**7a**) for comparison. Table II lists the lowest harmonic frequencies; complete frequency tables from outputs of calculations are given in the Supporting Information. The calculated dipole moments are presented in Table III.

Table IV collects the energies for structures of a multireference character. The effect of inclusion of the second reference on the heats of formation is shown in Table V. Table VI presents strain energies. They were estimated from the calculated enthalpies of structures **1**–**7**, ethane, and propane by means of the folowing isodesmic reactions.

$$C_5H_8\ (\mathbf{1}) + 8\ C_2H_6 \rightarrow 7\ C_3H_8$$

$$C_5H_6\ (\mathbf{2}\ \text{or}\ \mathbf{3}) + 11\ C_2H_6 \rightarrow 9\ C_3H_8$$

$$C_5H_4\ (\mathbf{4}\ \text{or}\ \mathbf{5}) + 14\ C_2H_6 \rightarrow 11\ C_3H_8$$

$$C_5H_2\ (\mathbf{6}) + 17\ C_2H_6 \rightarrow 13\ C_3H_8$$

$$C_5\ (\mathbf{7}) + 20\ C_2H_6 \rightarrow 15\ C_3H_8$$

Strain energies per C–C bond (strain energy divided by the number of C–C bonds shown in Fig. 1) are also presented. Heats of hydrogenation are shown in Table VII. Table VIII summarizes the results of NBO analysis of bonding in **1**–**7**.

In Figs 5–7, we present the calculated NMR, infrared, and Raman spectra. The vibrational spectra are unscaled. The scale for the Raman intensities of **1** and **2**, whose absolute values have not been determined, was set to fit

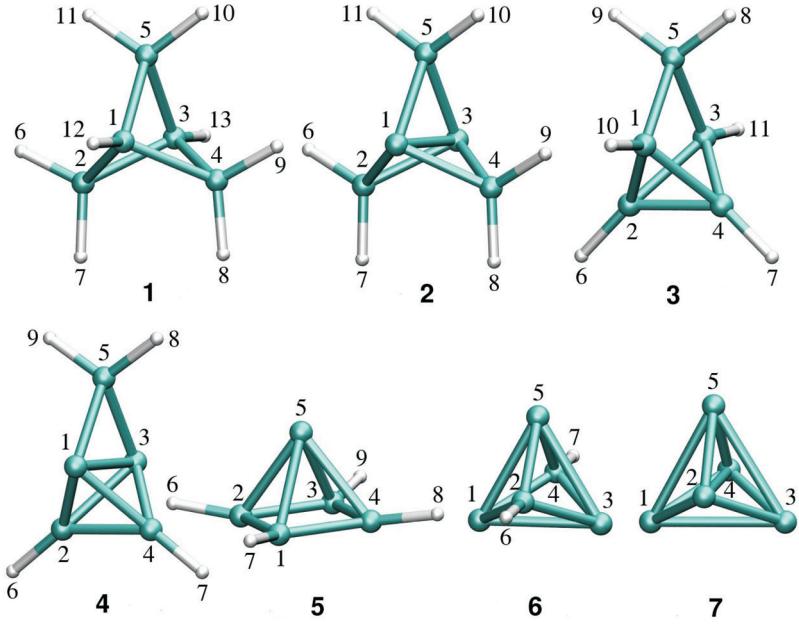

FIG. 1
Structures optimized at the CCSD(T)/cc-pVTZ level of theory

TABLE I
Geometry optimization results and total energies (in a.u.)[a]

Compd.	Sym.	Geom.	HF[c] 6-31G*	MP2[c] 6-31G*	B3LYP[d] 6-31G*	CCSD(T) cc-pVTZ	Exp.
1	D_{3h}	*r*[C(1)-C(2)]	1.546	1.549[d]	1.557	1.544	1.545[e], 1.557[f]
E = –195.00854		*r*[C(1)-C(3)]	1.870	1.873[d]	1.881	1.866	1.845[e], 1.874[f]
		r[C(2)-C(4)]	2.132	2.137[d]	2.149	2.130	2.147[e], 2.151[f]
		r[C(1)-H]	1.082			1.079	1.110[e], 1.109[f]
		r[C(2)-H]	1.085			1.084	1.110[e], 1.109[f]
		∠HC(2)H	111.0			112.4	103.9[e], 111.7[f]
2	D_{3h}	*r*[C(1)-C(2)]	1.503	1.514	1.518	1.508	1.512–1.555[g]
E = –193.76209		*r*[C(1)-C(3)]	1.544	1.592	1.580	1.572	1.593–1.605[g]
		r[C(2)-C(4)]	2.233	2.230	2.245	2.229	2.231–2.295[g]
		r[C(2)-H]	1.076	1.088		1.076	
		∠HC(2)H	118.7	114.9		115.96	
3	C_{2v}	*r*[C(1)-C(2)]	1.509	1.517	1.524	1.513	
E = –193.74668		*r*[C(1)-C(3)]	1.940	1.945	1.955	1.942	
		r[C(1)-C(5)]	1.534	1.535	1.543	1.529	
		r[C(2)-C(4)]	1.435	1.453	1.453	1.451	
		r[C(1)-H]	1.075	1.086		1.071	
		r[C(2)-H]	1.068	1.078		1.064	
		r[C(5)-H]	1.086	1.097		1.085	
		∠HC(5)H	110.7	111.0		111.7	
		∠HC(1)C(5)	132.4	132.9		126.5	
		∠HC(2)C(4)	137.6	136.7		136.7	
		∠C(5)C(1)C(3)C(2)[h]	141.6	141.4	141.6	141.3	
4	C_{2v}	*r*[C(1)-C(2)]	1.455	1.476	1.476	1.469	
E = –192.45990		*r*[C(1)-C(3)]	1.628	1.688	1.669	1.664	
		r[C(1)-C(5)]	1.508	1.516	1.520	1.508	
		r[C(2)-C(4)]	1.492	1.506	1.509	1.504	
		r[C(2)-H]	1.065	1.076		1.061	
		r[C(5)-H]	1.077	1.090		1.078	
		∠HC(2)C(4)	144.9	143.8		144.3	
		∠HC(5)H	114.8	114.6		115.5	
		∠C(5)C(1)C(3)C(2)[h]	141.8	141.5	141.7	141.6	

TABLE I
(*Continued*)

Compd.	Sym.	Geom.	HF[c] 6-31G*	MP2[c] 6-31G*	B3LYP[d] 6-31G*	CCSD(T) cc-pVTZ	Exp.
5	C_{4v}	*r*[C(1)-C(2)]	1.434	1.445	1.448	1.442	
E = –192.48200		*r*[C(1)-C(3)]	2.028	2.044	2.048	2.039	
		r[C(1)-C(5)]	1.620	1.645	1.659	1.639	
		r[C(1)-H]	1.068	1.080		1.066	
		∠HC(1)C(5)	121.3	119.4		120.7	
6	D_{3h}	*r*[C(1)-C(2)]	1.464	1.473	1.482	1.475	
E = –191.16941		*r*[C(1)-C(3)]	1.806	1.781	1.824	1.805	
		r[C(2)-C(4)]	2.056	2.109	2.084	2.086	
		r[C(2)-H]	1.066	1.077		1.063	
7	D_{3h}	*r*[C(1)-C(2)]	1.487[i]	1.489	1.497	1.492	
E = –189.81180		*r*[C(1)-C(3)]	1.710[i]	1.909	2.029	1.988	
		r[C(2)-C(4)]	2.107[i]	2.002	1.865	1.908	
7a[j]	$D_{\infty h}$	*r*[C(1)-C(2)]				1.288	
E = –189.93197		*r*[C(2)-C(3)]				1.276	

[a] Calculated at the CCSD(T) level for **1**, **3**, **5** and **6**, and at the MR BWCCSD(T) level for **2**, **4** and **7**; [b] lengths in Å, angles in °, for numbering of atoms, see Fig. 1; [c] ref.[6]; [d] ref.[19]; [e] ref.[47]; [f] ref.[48]; [g] see ref.[5] for further details and references to original papers; [h] dihedral angle; [i] at the HF level the D_{3h} structure is not stable; [j] linear C_5 isomer.

TABLE II
Lowest vibrational frequencies (in cm^{-1})

Compd.	Sym.	HF[a] 6-31G*	MP2[b] 6-31G*	CCSD(T) cc-pVTZ	Exp. results
1	*e′*	591	562	547	540[c]
2	*e′*	577	552	536	529[d]
3	b_2	512	479	464	
4	b_2	475	450	443	
5	*e′*	414	327	472	
6	*e′*	653	417	507	
7	*e′*	–[e]	508	541	

[a] Ref.[6]; [b] ref.[19]; [c] ref.[49]; [d] ref.[50]; [e] at the HF level the structure is not stable.

TABLE III
CCSD(T)/cc-pVTZ dipole moments (in D)[a]

Compd.	**1**	**2**	**3**	**4**	**5**	**6**	**7**
μ	0.0	0.0	0.46	0.18	1.84	0.0	0.0

[a] The positive end of the dipole is located at the bottom of the structure **3** and **5**, and at the top of structure **4**, as drawn in Fig. 1

TABLE IV
Total energies (excluding ZPE) for structures with significant multireference character (in a.u.)

Compd.	HF[a] 6-31G*	MP2[b] 6-31G*	CCSD(T) cc-pVTZ	MR BWCCSD(T) cc-pVTZ
2	–192.69107	–193.37471	–193.75928	–193.76209
4	–191.42314	–192.10369	–192.45645	–192.45990
7	–188.83663	–189.51932	–189.80672	–189.81180

[a] Ref.[6]

TABLE V
CCSD(T)/cc-pVTZ and MR BWCCSD(T)/cc-pVTZ heats of formation and ZPE (in kcal/mol)

Compd.	HF/6-31G*[a]	CCSD(T)/cc-pVTZ		MR BWCCSD(T)/cc-pVTZ		ZPE
	$\Delta_f H^o$(298 K)	$\Delta_f H^o$(0 K)	$\Delta_f H^o$(298 K)	$\Delta_f H^o$(0 K)	$\Delta_f H^o$(298 K)	
1	50.4	51.3	45.1			74.3
2	88.5	89.6	85.4	87.9	83.6	59.2
3	96.0	96.4	92.2			58.1
4	164.0	160.4	158.1	158.3	155.9	43.0
5	143.0	144.1	141.9			42.7
6	222.6	221.6	221.3			27.1
7	–[b]	329.4	331.1	326.2	327.9	10.3

[a] Ref.[6]; [b] at the HF level the structure is not stable.

the most intense calculated peak. Tables IX and X collect the NMR indirect spin-spin coupling constants.

Vertical and adiabatic excitation energies to the lowest triplet state of **1**–**7** are listed in Table XI. Optimization of the geometry of the triplet state, starting at the optimal singlet geometry, yielded the structures shown in Fig. 2, which also summarizes the most important geometrical parameters of the triplet structures. In the case of **1**, triplet optimization within the D_{3h} point group led to a saddle point with two imaginary frequencies. Follow-

TABLE VI
Strain energies from calculated[a] isodesmic reaction enthalpies (in kcal/mol)

Compd.	ΔH^o (0 K)	ΔH^o (298 K)	ΔH^o (298 K)/C-C[b]
1	62.0	63.1	10.5 (63.1/6)
2	90.8	93.4	13.3 (93.4/7)
3	99.4	102.0	14.6 (102.0/7)
4	153.5	157.4	19.7 (157.4/8)
5	139.3	143.4	17.9 (143.4/8)
6	209.3	214.6	23.8 (214.6/9)
7	306.0	312.7	31.3 (312.7/10)

[a] CCSD(T)/cc-pVTZ for **1**, **3**, **5** and **6**, and MR BWCCSD(T)/cc-pVTZ for **2**, **4** and **7**; [b] Strain energies divided by the number of formal C–C bonds shown in Fig. 1

TABLE VII
Heats of hydrogenation from calculated enthalpies[a] (in kcal/mol)

Reaction	ΔH^o (0 K)	ΔH^o (298 K)
2 + H_2 → **1**	–37.66	–37.67
3 + H_2 → **1**	–46.25	–46.30
4 + H_2 → **2**	–71.52	–71.46
4 + H_2 → **3**	–62.93	–62.83
5 + H_2 → **3**	–48.74	–48.79
6 + H_2 → **5**	–78.77	–78.56
6 + H_2 → **4**	–64.58	–64.53
7 + H_2 → **6**	–105.56	–105.59

[a] CCSD(T)/cc-pVTZ for **1**, **3**, **5** and **6**, and MR BWCCSD(T)/cc-pVTZ for **2**, **4** and **7**.

TABLE VIII
Results of NBO analysis

Compd.[a]	NBO[b]	Occ.[c]	NHO 1				NHO 2			
			Cent.	Coef.[d]	Char.	Dev.[e]	Cent.	Coef.	Char.	Dev.
1	BD 1	1.93	C(1)	0.71	$sp^{3.28}$	20 °	C(2)	0.70	sp3.34	18 °
97.9%	BD 2	1.96	C(1)	0.78	$sp^{2.37}$		H	0.63	s	
	BD 3	1.96	C(2)	0.77	$sp^{2.70}$		H	0.64	s	
2	BD 1	1.92	C(1)	0.72	$sp^{1.99}$	33 °	C(2)	0.70	$sp^{3.61}$	23 °
97.7%	BD 2	1.80	C(1)	0.71	$sp^{99.99}$	0 °	C(3)	0.71	$sp^{99.99}$	0 °
	BD 3	1.96	C(2)	0.78	$sp^{2.53}$		H	0.63	s	
3	BD 1	1.91	C(1)	0.70	$sp^{4.14}$	28 °	C(2)	0.71	$sp^{3.32}$	30 °
97.7%	BD 2	1.94	C(1)	0.71	$sp^{2.58}$	16 °	C(5)	0.70	$sp^{3.17}$	16 °
	BD 3	1.91	C(2)	0.71	$sp^{4.99}$	31 °	C(4)	0.71	$sp^{4.99}$	31 °
	BD 4	1.96	C(1)	0.78	$sp^{2.03}$		H	0.62	s	
	BD 5	1.96	C(2)	0.79	$sp^{1.72}$		H	0.61	s	
	BD 6	1.95	C(5)	0.77	$sp^{2.83}$		H	0.64	s	
4	BD 1	1.91	C(1)	0.70	$sp^{2.52}$	34 °	C(2)	0.71	$sp^{3.51}$	27 °
96.9%	BD 2	1.77	C(1)	0.71	$sp^{36.88}$	4 °	C(3)	0.71	$sp^{36.88}$	4 °
	BD 3	1.91	C(1)	0.73	$sp^{1.41}$	32 °	C(5)	0.69	$sp^{3.51}$	19 °
	BD 4	1.90	C(2)	0.71	$sp^{4.88}$	33 °	C(4)	0.71	$sp^{4.88}$	33 °
	BD 5	1.96	C(2)	0.79	$sp^{1.60}$		H	0.61	s	
	BD 6	1.95	C(5)	0.78	$sp^{2.58}$		H	0.63	s	
5	BD 1	1.59	C(1)	0.75	$sp^{15.72}$	21 °	C(5)	0.66	$sp^{6.06}$	22 °
95.0%	BD 2	1.59	C(3)	0.75	$sp^{15.72}$	21 °	C(5)	0.66	$sp^{6.06}$	22 °
	BD 3	1.60	C(2)	0.75	$sp^{15.72}$	21 °	C(5)	0.67	$sp^{33.21}$	38 °
	BD 4	1.93	C(5)	1	$sp^{0.44}$					
	BD 5	1.94	C(1)	0.71	$sp^{2.43}$	24 °	C(2)	0.71	$sp^{2.43}$	24 °
	BD 6	1.94	C(1)	0.71	$sp^{2.43}$	24 °	C(4)	0.71	$sp^{2.78}$	29 °
	BD 7	1.96	C(4)	0.79	$sp^{1.90}$		H	0.61	s	
	BD 8	1.96	C(2)	0.79	$sp^{1.81}$		H	0.61	s	
	BD 9	1.96	C(1)	0.79	$sp^{1.81}$		H	0.61	s	
6	BD 1	1.86	C(1)	0.71	$sp^{1.15}$	32 °	C(2)	0.71	$sp^{3.43}$	21 °
93.7%	BD 2	1.64	C(1)	0.71	$sp^{24.70}$	19 °	C(3)	0.71	$sp^{24.70}$	19 °
	BD 3	1.96	C(2)	0.80	$sp^{2.08}$		H	0.60	s	
7	BD 1	1.77	C(1)	0.65	$sp^{5.04}$	14 °	C(2)	0.76	$sp^{2.20}$	31 °
92.0%	LP 2	1.75	C(1)	1	$sp^{0.49}$					
	BD 3	1.72	C(2)	0.71	$sp^{13.15}$	0 °	C(4)	0.71	$sp^{13.15}$	0 °

[a] Per cent weight of the dominant Lewis structure; [b] type of a natural bond orbital (NBO), BD denotes 2-center bond, LP denotes lone pair; [c] occupation of NBO; [d] coefficient of a natural hybrid orbital (NHO) in NBO; [e] angle between orbital axis and internuclear line.

TABLE IX
Spin-spin coupling constants in **1–3** (in Hz)

1			**2**			**3**				
Coupl. const.	CCSD IGLO-III	Exp.[a] |J|	Coupl. const.	CCSD IGLO-III	Exp.[a] |J|	Coupl. const.	CCSD IGLO-III	Exp.[a] |J|	Coupl. const.	CCSD IGLO-III
$^{1}J_{C1C2}$	25.07	25.1	$^{1}J_{C1C2}$	10.73	9.9[d]	$^{1}J_{C1C2}$	18.79	19.0	$^{2}J_{C5H10}$	–0.11
$^{2}J_{C1C3}$	–27.52	25.1[b]	$^{1}J_{C1C3}$	18.59	0.6[b]	$^{2}J_{C1C3}$	–16.97		$^{3}J_{H6H7}$	1.39
$^{2}J_{C2C4}$	–5.37	5.2[b]	$^{2}J_{C2C4}$	–0.61		$^{1}J_{C1C5}$	30.86	34.0	$^{4}J_{H6H8}$	0.91
$^{2}J_{C1H6}$	–2.99	3	$^{2}J_{C1H6}$	–0.89		$^{1}J_{C2C4}$	–1.8		$^{4}J_{H6H9}$	–0.06
$^{1}J_{C1H12}$	146.33	167.8	$^{1}J_{C2H6}$	147.21	163.7[d]	$^{2}J_{C2C5}$	–4.52		$^{3}J_{H6H10}$	–0.58
$^{3}J_{C1H13}$	11.12	10.0	$^{3}J_{C2H8}$	4.22		$^{2}J_{C1H6}$	0.49		$^{2}J_{H8H9}$	–4.02
$^{1}J_{C2H6}$	129.54	144.5	$^{3}J_{C2H9}$	15.15		$^{2}J_{C1H8}$	–4.15		$^{3}J_{H9H10}$	0.30
$^{3}J_{C2H8}$	7.05	7.8	$^{2}J_{H6H7}$	–2.75		$^{1}J_{C1H10}$	164.81		$^{4}J_{H10H11}$	11.09
$^{3}J_{C2H9}$	14.78	15.5	$^{4}J_{H6H8}$	0.33		$^{3}J_{C1H11}$	10.95			
$^{2}J_{C2H12}$	0.15	0[c]	$^{4}J_{H6H9}$	5.08		$^{1}J_{C2H6}$	102.41	210		
$^{2}J_{H6H7}$	–2.63		$^{4}J_{H7H8}$	–0.22		$^{2}J_{C2H7}$	–1.50			
$^{4}J_{H6H8}$	0.12	0[c]				$^{3}J_{C2H8}$	18.86			
$^{4}J_{H6H9}$	7.23	9.6				$^{3}J_{C2H9}$	5.25			
$^{4}J_{H7H8}$	–0.32	0[c]				$^{2}J_{C2H10}$	0.09			
$^{3}J_{H6H12}$	0.15	0[c]				$^{3}J_{C5H6}$	–0.42			
$^{4}J_{H12H13}$	14.03	18.2				$^{1}J_{C5H8}$	123.52			

[a] Ref.[51] unless stated otherwise; [b] ref.[52], average of values for alkyl substituted compounds (see ref.[13]); [c] too small to be observed; [d] ref.[53]; [e] ref.[4]

TABLE X
Spin-spin coupling constants in **4**–**7** (in Hz)

4		**5**		**6**		**7**	
Coupl. const.	CCSD IGLO-III	Coupl. const.	CCSD IGLO-III	Coupl. const.	CCSD IGLO-III	Coupl. const.	CCSD IGLO-III
$^{1}J_{C1C2}$	4.52	$^{1}J_{C1C2}$	37.79	$^{1}J_{C1C2}$	–1.38	$^{1}J_{C1C2}$	–10.82
$^{1}J_{C1C3}$	34.34	$^{2}J_{C1C3}$	–2.82	$^{1}J_{C1C3}$	–3.97	$^{2}J_{C1C3}$	14.19
$^{1}J_{C1C5}$	10.79	$^{1}J_{C1C5}$	–18.88	$^{2}J_{C2C4}$	0.31	$^{1}J_{C2C4}$	233.95
$^{1}J_{C2C4}$	1.76	$^{2}J_{C1H6}$	1.11	$^{2}J_{C1H6}$	5.82		
$^{2}J_{C2C5}$	–3.13	$^{1}J_{C1H7}$	136.50	$^{1}J_{C2H6}$	141.26		
$^{2}J_{C1H6}$	6.14	$^{3}J_{C1H9}$	11.63	$^{3}J_{C2H7}$	15.81		
$^{2}J_{C1H8}$	–3.51	$^{2}J_{C5H6}$	4.98	$^{4}J_{H6H7}$	–2.72		
$^{1}J_{C2H6}$	153.47	$^{3}J_{H6H7}$	–1.27				
$^{2}J_{C2H7}$	–2.85	$^{4}J_{H6H8}$	4.12				
$^{3}J_{C2H8}$	17.99						
$^{3}J_{C2H9}$	3.27						
$^{3}J_{C5H6}$	–1.41						
$^{1}J_{C5H8}$	142.81						
$^{3}J_{H6H7}$	–2.22						
$^{4}J_{H6H8}$	0.30						
$^{4}J_{H6H9}$	1.31						
$^{2}J_{H8H9}$	–3.51						

ing one of them produced the biradical structure **1** presented in Fig. 2. The second one led to the structure **1a** (Fig. 3), which is 31.1 kcal/mol higher in energy. Further search on the triplet surface identified the minima **1b** and **1c** shown in Fig. 3. In the case of **4**, geometry optimization of the triplet state yielded the structure **4′** shown in Fig. 2. Further search produced the minimum **4″**, more stable by 24.3 kcal/mol. Similar situation was found also in the case of **6**. Geometry optimization yielded the structure **6′** and further search discovered the minimum **6″**, more stable by 11.9 kcal/mol.

Finally, we have investigated the thermal isomerization of **3** to **8** (Scheme 2), and the results are summarized in Tables XII and XIII. Table XII compares the activation and reaction enthalpies calculated at different levels of theory, and Table XIII gives the vertical singlet-triplet gaps (ΔE = $E_{\text{triplet}} - E_{\text{singlet}}$). Our calculations agreed that at the geometry of the TS (Fig. 4), the singlet-triplet gap is negative[15], with the triplet state below the singlet. Selected interatomic distances of the optimized geometries of the singlet transition state at the CASPT2(4,4) and CASSCF(8,8) levels are compared in Fig. 4.

TABLE XI
Vertical (vert.) and adiabatic (adiab.) excitation energies (in eV) to the lowest triplet state

Compd.	(U)MP2(FC)/cc-pVTZ		ROHF-CCSD(T)/cc-pVTZ
	ΔE_{S-T}(vert.)	ΔE_{S-T}(adiab.)	ΔE_{S-T}(vert.)
1	9.115	2.548[a]	10.098
2	5.267	4.597	4.934
3	8.302	2.920	7.909
4′	4.449	3.318	4.947
4″	4.449	2.266	4.947
5	6.946	3.537[a]	7.579
6′	4.223	2.325[a]	3.908
6″	4.223	1.808[a]	3.908
7	2.994	1.443[a]	3.768

[a] Symmetries of the singlet and triplet states are different (Fig. 2).

TABLE XII
Activation and reaction enthalpies for thermal isomerization of **3** to **8** (in kcal/mol)

	$\Delta^{\ddagger}H^{o}$(298 K)	$\Delta_r H^{o}$(298 K)
CASSCF(4,4)/6-31G(d)[a]	33.8	–79.0
CASSCF(8,8)/6-31G(d)[a]	39.0	–79.5
CASSCF(8,8)-MP2/6-31G(d)[a,b]	40.5	–66.9
CR-CCSD(T)/6-31G(d)[a,c]	48.3	–63.7
CASPT2(4,4)/cc-pVTZ	43.0	–62.0
MR BWCCSD/cc-pVTZ	47.8[d]	–58.2[e]
MR BWCCSD(T)/cc-pVTZ	43.5[d]	–58.7[e]

[a] Ref.[15]; [b] calculated at the CASSCF(8,8) optimized geometries with CASSCF(8,8) ZPEs and thermal corrections; [c] calculated at the (U)B3LYP optimized geometries with (U)B3LYP ZPEs and thermal corrections; [d] TS calculated at the CASPT2(4,4) optimized geometries with CASPT2(4,4) ZPEs and thermal corrections; [e] **8** calculated at the single-reference coupled cluster (SR-CC) optimized geometries with SR-CC ZPEs and thermal corrections.

TABLE XIII
Vertical singlet-triplet separation energies of transition state (in kcal/mol)

	ΔE_{S-T}
UB3LYP/6-31G(d)[a]	2.7
CASSCF(4,4)/6-31G(d)[a]	–1.5
CASSCF(8,8)/6-31G(d)[a]	–2.3
CASSCF(8,8)-MP2/6-31G(d)[a,b]	–3.0
CASPT2(4,4)/cc-pVTZ	–2.4
MR BWCCSD/cc-pVTZ	–1.5
MR BWCCSD(T)/cc-pVTZ	–2.2

[a] Ref.[15]; [b] calculated at the CASSCF(8,8) optimized singlet geometry; [c] calculated at the CASPT2(4,4) optimized singlet geometry.

DISCUSSION

Perhaps the most striking result of the present study is the similarity of the conclusions to those obtained earlier[6] with the MP2/6-31G* method.

*Bonding in **1**–**7***

The differences in the bond lengths and valence angles calculated with the different methods are small (Table I). The experimental results available for **1** and **2** agree with the calculations quite well but their uncertainty is too large to permit a convincing claim of higher accuracy for the CCSD(T) results. In the case of **7**, the CCSD(T) result agrees with MP2 and DFT in pre-

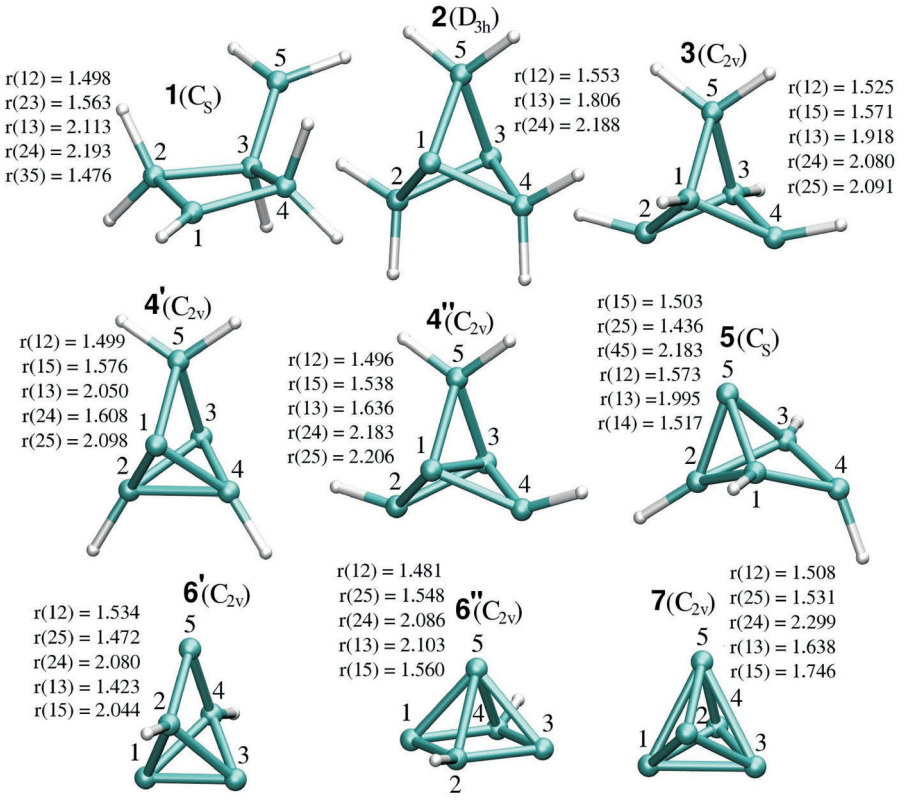

FIG. 2
Triplet state structures of **1**–**7** optimized at the UMP2(FC)/cc-pVTZ level together with selected interatomic distances in Å

dicting the D_{3h} structure to be a local minimum on the potential energy surface, and the HF result seems to be unreliable.

As expected for small-ring compounds, C–C bonds have an increased p character and C–H bonds an increased s character relative to sp^3. In **1**, whose bonding is fairly unexceptional, the bridge carbon uses an $sp^{3.34}$ hybrid for C–C bonds and $sp^{2.70}$ hybrid for C–H bonds, and for the bridgehead carbon, these hybrids are $sp^{3.28}$ and $sp^{2.37}$, respectively.

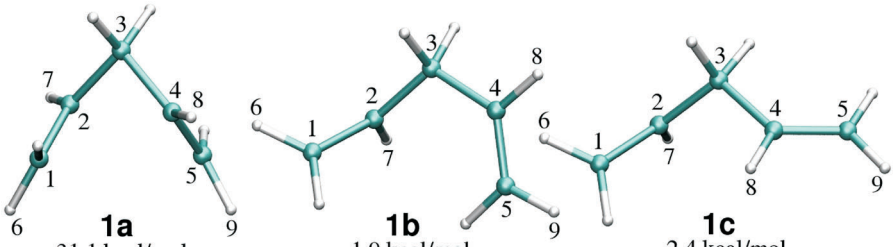

FIG. 3

Additional triplet state structures derived from **1**, optimized at the UMP2(FC)/cc-pVTZ level, and their energies relative to triplet **1** (Fig. 2); d denotes dihedral angle

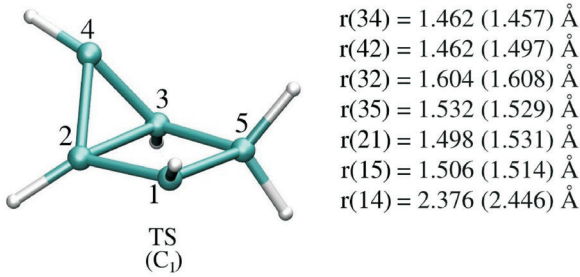

FIG. 4

Selected interatomic distances in the transition state (TS) of the thermal isomerization of tricyclo[2.1.0.$0^{2,5}$]pentane (**3**) to 1,3-cyclopentadiene (**8**) from CASPT2(4,4)/cc-pVTZ and CASSCF(8,8)/cc-pVTZ (in parentheses) optimization

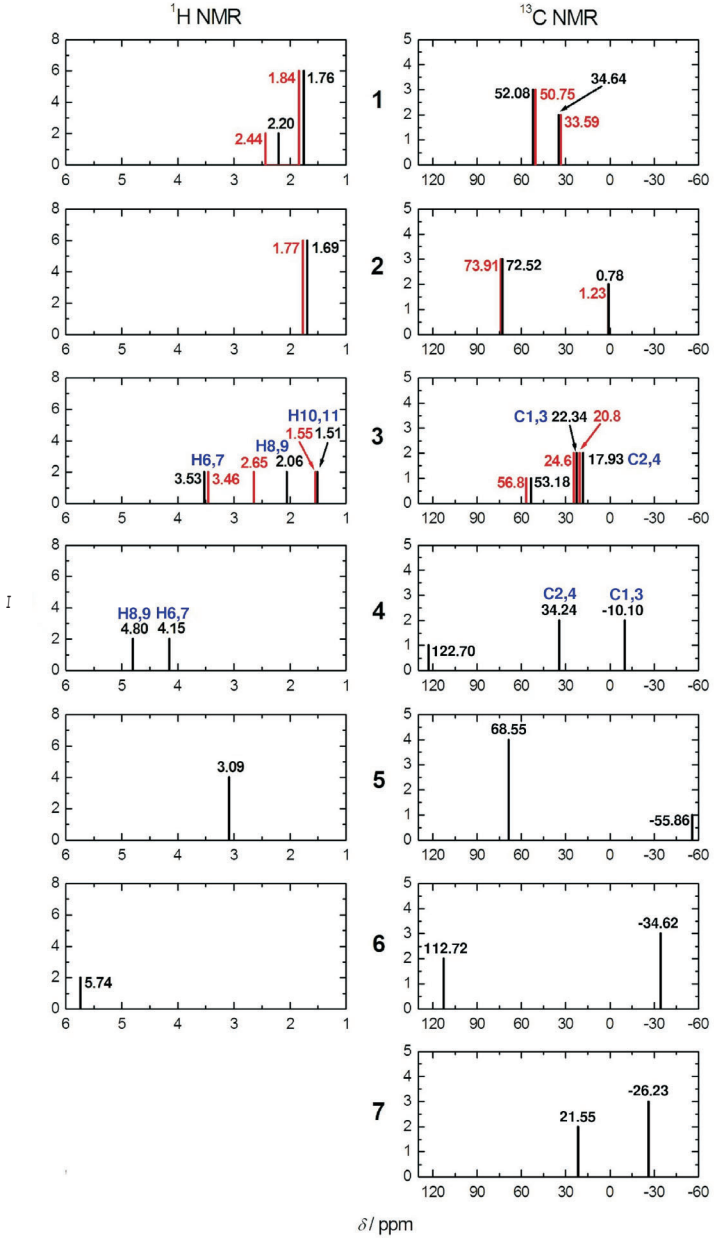

FIG. 5

NMR spectra of **1**–**7**. Black: CCSD(T)/cc-pVTZ, red: experimental[3,4,54,55]. Intensity reflects the number of equivalent atoms

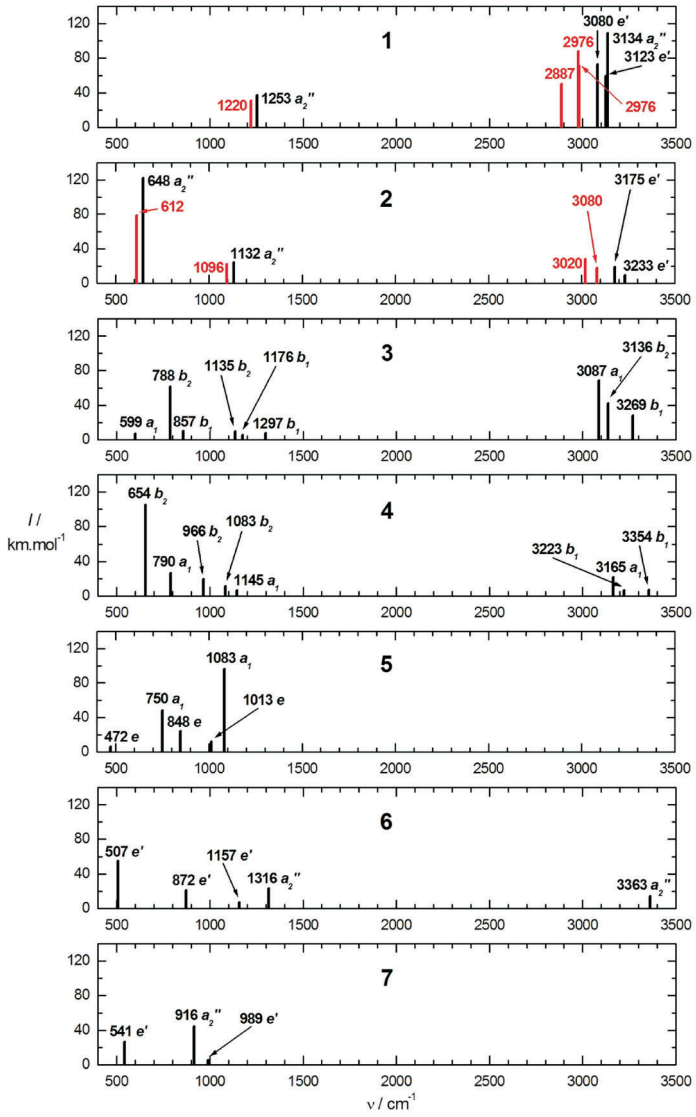

FIG. 6
Infrared spectra of **1**–**7**. Black: CCSD(T)/cc-pVTZ, red: experimental[49,50]

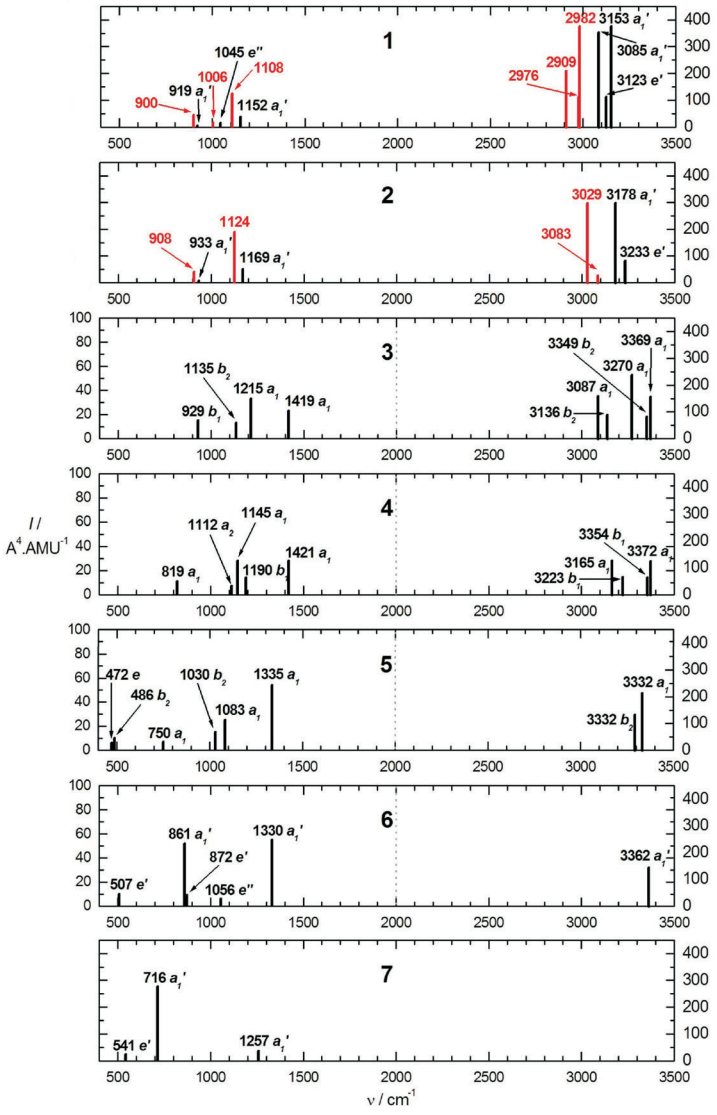

FIG. 7

Raman spectra of **1**–**7**. Black: MP2/cc-pVTZ intensities assigned to CCSD(T)/cc-pVTZ frequencies, red: experimental[50,56]. For **3**–**6** the left intensity scale applies below 2000 cm^{-1} and the right scale above 2000 cm^{-1}

Structures **2**–**6** are derived from **1** by the induction of inter-bridgehead (IH) and inter-bridge (IB) bonds, which have similar characteristics in all of the compounds. The IH bonds tend to be longer (1.57 Å in **2**, 1.66 Å in **4**, and 1.91 Å in **7**) than IB bonds (1.45 Å in **3**, 1.50 Å in **4**, 1.64 Å in **5**, and 1.81 Å in **6**). In **7** the IB bonds are only formally present and the real structure is that of a tricarbene. Surprisingly, although longer, the IH bonds tend to be stronger. Their hydrogenation energies are –37.7 kcal/mol in **2** and –62.8 kcal/mol in **4**, whereas for the IB bonds the values are –46.3 kcal/mol in **3**, –71.5 kcal/mol in **4**, –48.8 kcal/mol in **5**, and –78.6 in **6**. Hence, **2** is 9.7 kcal/mol more stable than its isomer **3**. Energies needed for adiabatic conversion into a triplet biradical are 106.0 kcal/mol in **2**, 76.5 kcal/mol in **4** and 33.3 kcal/mol in **7**, when breaking an IH bond, and 67.3 kcal/mol in **3**, 52.3 kcal/mol in **4**, 81.6 kcal/mol in **5** and 41.7 kcal/mol in **6**, when breaking an IB bond.

The natural hybrid orbitals (NHOs) used by the bridgehead atoms to form IH bonds are nearly purely p in character, as was recognized earlier[5]. Their occupancies are relatively low (1.7–1.8) and those of the corresponding antibond relatively high (~0.2), indicating partial biradicaloid character. They delocalize fairly strongly into the neighbouring bonds. The NHOs used by the bridge atoms to form IB bonds are of only somewhat lower p character ($sp^{4.99}$ in **3**, $sp^{4.88}$ in **4**, and nearly pure p in **5** and **6**). The axes of the IB bonds deviate by 20–30° from the line connecting the nuclei, showing that the IB bonds are strongly bent. The IH bonds are bent very little or not at all.

The weight of the dominant Lewis structure drops from 98% for **1** to 92% in **7**. The best structure for **7** is a tricarbene, and the lone pairs at three bridges have 67% s character. There is no IB bonding. A similar result is obtained for **6** at the Hartree–Fock, but not at the correlated level of calculation. The dipole moments of these hydrocarbons are small with the remarkable exception of **5**, which carries a lone pair on the apical carbon and can be viewed as a result of interaction of a C^{2-} dianion with a cyclobutadiene dication. This has been pointed out previously[9] and the chemical consequences analyzed in great detail[10].

Strain energies are high for all of these compounds but those for **6** and **7** stand out as especially high. Heats of hydrogenation at 0 and 298 K are nearly the same (Table VII), as the thermal corrections largely cancel. The heat of hydrogenation which yields **6** from **7** is also very high. There is probably only very little hope that **7** could be synthesized, since this D_{3h} isomer of C_5 is 78.6 kcal/mol higher in energy (at the CCSD(T) level) than the most stable linear isomer[39–42].

Vibrational Spectra

The trend in the series HF, MP2 and CCSD(T) is as expected (Table II) and the latter methods yield better agreement with the frequencies observed in **1** and **2**. The lowest frequencies of the seven compounds do not differ substantially. They are relatively high and do not indicate unimolecular instability. The agreement of calculated peak positions with the available experimental spectra of **1**–**3** is good enough to trust the predictions for **4**–**7**. The calculated vibrational frequencies are somewhat higher than those observed, as is usual for harmonic calculations. The calculated intensities agree less well, especially in the case of Raman.

NMR Spectra

The ^{1}H NMR chemical shifts agree within 0.25 ppm, except for the CH_2 protons in **3**, which are off by 0.6 ppm. The ^{13}C NMR shifts agree within 3.6 ppm, and in most cases even better.

The agreement between calculated and experimental indirect spin-spin coupling constants of **1**, **2**, and **3** is generally quite good. It is worst for single-bond carbon–hydrogen coupling constants $^{1}J_{CH}$, which are generally calculated about 15–20 Hz smaller than they should be, similarly as in previous reports[13,43,44]. We therefore expect the constants calculated for **4**–**7** to be underestimated as well. We are puzzled by the very striking disagreement in the case of the $^{1}J_{C2H6}$ coupling constant in **3**, where the calculated value is 100 Hz lower than the reported experimental number.

Carbon–carbon coupling constants agree nicely with experimental results except the case of $^{1}J_{C1C3}$ in **2**. This coupling constant was already discussed in ref.[13], where only the FC contribution to this coupling constant was calculated at the CCSD level of theory, and it was suggested that the disagreement between experimental and calculated value might be caused by large solvent or substituent effects. Our result, which includes all four contributions at the CCSD level, is in slightly better agreement with experiment, but the discrepancy with experimental value is still 18 Hz.

Generally speaking all the spin-spin coupling constants are dominated by the FC term. For the H–H coupling constants, the large PSO and DSO terms almost cancel, as is usual. The only relatively large SD contributions are present in the $^{1}J_{C1C3}$ coupling constants in **2** and **4**, which confirm the similar nature of these bonds. Relatively large SD and PSO contributions are also present in the $^{1}J_{C1C3}$ coupling constant in **6**, and in the $^{2}J_{C1C3}$ and $^{1}J_{C2C4}$ coupling constants in **7**.

Finally, it has already been pointed out[13] that the large change in $^1J_{C1C3}$ from **1** to **2** indicates a very different character of the coupling path in these molecules and confirms the existence of the IH bond. Here we add that the same is true also for **3** and **4**, as is expected.

Triplet States

A small vertical singlet-triplet separation would be an indication of biradicaloid character and probable chemical instability, but is not observed even in the most highly strained compounds. Optimization of the triplet structures led to triplet biradicals, which differ from the starting singlet ground state by the loss of one C–C bond. Optimization on the triplet surfaces of **2**, **3**, and **4** leads to local minima of the same molecular symmetry as the starting singlet ground states. The observed[45] vertical (4.70 eV) excitation energy of **2** agrees quite nicely with our CCSD(T) result (4.93 eV) but the observed adiabatic (4.19 eV) excitation energy agrees less well with the MP2 result (4.60 eV).

When the triplet state geometry optimization of **4** was started at the geometry of the singlet ground state, it produced a biradical structure, in which the IH C(1)–C(3) bond was broken (Fig. 2). The structure **4″** with the C(2)–C(4) bond broken is nevertheless 24.3 kcal/mol lower in energy than the structure **4′** with the C(1)–C(3) bond broken. In a similar fashion, optimization of the triplet of **6**, starting at the equilibrium geometry of the singlet, led to the carbene structure **6′**, in which two IB bonds have been lost. Further search identified the more stable 1,3-biradical structure **6″**, in which only one IB bond has been broken.

The structure **1a** is a triplet state of 1,4-pentadiene with excitation equally shared by both double bonds, which are twisted by ~23°. The SCF atomic spin density is ~0.5 at each carbon atom of each double bond. It represents an intermediate for triplet energy transfer from one to the other isolated double bond of 1,4-pentadiene with excitation localized on one of the double bonds (**1b** in Fig. 3), which is 33.0 kcal/mol lower than **1a**. In **1b**, one double bond is planar and carries no spin density, while the other is twisted by ~90° and each of its carbons carries a spin density of ~1. The structure **1c** from Fig. 3 is a slightly more stable conformer of **1b**. It is possible that at a higher level of calculation the local minimum **1a** will become a transition state for the triplet energy transfer.

*Thermal Rearrangement of **3***

The hydrocarbon **3** is known to open thermally to **8**. Although the mechanism of this "symmetry-forbidden" process is intriguing, no kinetic study has been performed. It has been shown[16] at the MCSCF(10,10)/6-31G(d,p) level that the Woodward–Hoffmann allowed conrotatory process, which would require an intermediate formation of (*E*,*Z*)-1,3-cyclopentadiene, does not occur, and that (*E*,*Z*)-1,3-cyclopentadiene is not a stable structure. The reaction path that is followed proceeds through a biradicaloid transition state and single reference methods such as MP2 or CCSD(T) fail to locate it[16]. This reaction is thus a good candidate for testing the performance of various multireference methods.

It has been pointed out[15] that the CASSCF method probably overestimates the multireference character of the TS, which results in an excessive length of one of the breaking bonds (r_{14} = 2.446 Å). Our CASPT2 calculation, which recovers static as well as dynamic correlation and should predict a more reliable geometry for the TS, reduces this distance to 2.376 Å. This value is nevertheless still higher than in the final structure, 1,3-cyclopentadiene (2.29 Å [46]).

The results of the various approximations (Table XII) are consistent and show a trend indicating that the MR BWCCSD(T) value is the most reliable, and that the CR-CCSD(T)/(U)B3LYP approach probably overestimates the activation enthalpy. Our best predictions from MR BWCCSD(T) calculations are 43.5 kcal/mol for activation enthalpy and –58.7 kcal/mol for reaction enthalpy.

CONCLUSIONS

The previous conclusion that **1**–**7** represent potential energy surface minima has now been confirmed at a higher level of theory, CCSD(T)/cc-pVTZ, with explicit consideration of multireference character where required, and NMR, IR and Raman spectroscopic properties for the presently unknown members of the series have been predicted. Triplet surfaces of these strained hydrocarbons have been computed at the UMP2/cc-pVTZ level of theory, and an interesting intermediate (or possibly, a transition state) for triplet energy transfer from one to the other double bond of 1,4-pentadiene has been identified.

Supporting Information

Optimized geometries of **1**–**7**, TS and **8**, complete frequency tables of **1**–**7**, ^{1}H and ^{13}C NMR shielding tensors of **1**–**7** and methane are available on the web: http://dx.doi.org/10.1135/cccc20081525.

This work has been supported by the COST D37 action, the Czech Science Foundation (203/07/0070), the Grant Agency of the Academy of Sciences of the Czech Republic (1EY400400413), and the U.S. NSF (CHE-0446688 and OISE 0532040).

REFERENCES

1. Freund A. J.: *Prakt. Chem.* **1882**, *26*, 367.
2. Wiberg K. B., Walker F. H.: *J. Am. Chem. Soc.* **1982**, *104*, 5239.
3. Wiberg K. B., Connor D. S.: *J. Am. Chem. Soc.* **1966**, *88*, 4437.
4. Andrews G. D., Baldwin J. E.: *J. Am. Chem. Soc.* **1977**, *99*, 4851.
5. Levin M. D., Kaszynski P., Michl J.: *Chem. Rev.* **2000**, *100*, 169.
6. Balaji V., Michl J.: *Pure Appl. Chem.* **1988**, *60*, 189.
7. Gund P., Gund T. M.: *J. Am. Chem. Soc.* **1981**, *103*, 4458.
8. Ekholm M., Nevalainen V., Pyykkö P.: *Finn. Chem. Lett.* **1989**, *16*, 107.
9. Lewars E.: *J. Mol. Struct. (THEOCHEM)* **1998**, *423*, 173.
10. Lewars E.: *J. Mol. Struct. (THEOCHEM)* **2000**, *507*, 165.
11. Jarosch O., Walsh R., Szeimies G.: *J. Am. Chem. Soc.* **2000**, *122*, 8490.
12. Kenny J. P., Krueger K. M., Rienstra-Kiracofe J. C., Schaefer H. F.: *J. Phys. Chem. A* **2001**, *105*, 7745.
13. Pecul M., Dodziuk H., Jaszuński M., Lukin O., Leszczyński J.: *Phys. Chem. Chem. Phys.* **2001**, *3*, 1986.
14. Ebrahimi A., Deyhimi F., Roohi H.: *J. Mol. Struct. (THEOCHEM)* **2003**, *626*, 223.
15. Özkan I., Kinal A., Balci M.: *J. Phys. Chem. A* **2004**, *108*, 507.
16. Davis S. R., Qin C. Y., Zhao Z. D.: *Int. J. Quantum Chem.* **2004**, *96*, 411.
17. Krivdin L. B.: *Magn. Reson. Chem.* **2004**, *42*, 1.
18. Polo V., Andres J., Silvi B.: *J. Comput. Chem.* **2006**, *28*, 857.
19. Lewars E.: *Modelling Marvels. Computational Anticipation of Novel Molecules*. Chap. 13. Springer, Netherlands 2008.
20. Dunning T. H.: *J. Chem. Phys.* **1989**, *90*, 1007.
21. https://bse.pnl.gov/bse/portal (8. 4. 2008).
22. Helgaker T., Jaszuński M., Ruud K.: *Chem. Rev.* **1999**, *99*, 293.
23. Schindler M., Kutzelnigg W.: *J. Chem. Phys.* **1982**, *76*, 1919.
24. Demel O., Pittner J.: *J. Chem. Phys.* **2006**, *124*, 144112.
25. Hubač I., Pittner J., Čársky P.: *J. Chem. Phys.* **2000**, *112*, 8779.
26. Chase M. W., Davies C. A., Downey J. R., Frurip D. J., McDonald R. A., Syverud A. N.: *J. Phys. Chem. Ref. Data* **1985**, *14*, 1.
27. Lacey M. J., Macdonald C. G., Pross A., Shannon J. S., Sternhell S.: *Aust. J. Chem.* **1970**, *23*, 1421.

28. Pretsch E., Clerc T., Seibl J., Simon W.: *Tabellen zur Strukturaufklärung Organischer Verbindungen mit Spektroskopischen Methoden*. Springer, Berlin 1976.
29. http://www.aces2.de (8. 7. 2008).
30. Pittner J., Šmydke J., Čársky P., Hubač I.: *J. Mol. Struct. (THEOCHEM)* **2001**, *547*, 239.
31. Pittner J., Nachtigall P., Čársky P., Hubač I.: *J. Phys. Chem. A* **2001**, *105*, 1354.
32. Pittner J.: *J. Chem. Phys.* **2003**, *118*, 10876.
33. Stanton J., Gauss J., Watts J., Nooijen M., Oliphanta N., Perera S., Szalay P., Lauderdale W., Kucharski S., Gwaltney S., Beck S., Balková A., Bernholdt D., Baeck K., Rozyczko P., Sekino H., Hober C., Bartlett R.: *ACES II*, A Program Product of the Quantum Theory Project, University of Florida. Integral packages included are: *VMOL* (J. Almlöf and P. R. Taylor), *VPROPS* (P. Taylor), *ABACUS* (T. Helgaker, H. J. Aa. Jensen, P. Jørgensen, J. Olsen and P. R. Taylor).
34. Werner H.-J., Knowles P. J., Lindh R., Manby F. R., Schütz M., Celani P., Korona T., Rauhut G., Amos R. D., Bernhardsson A., Berning A., Cooper D. L., Deegan M. J. O., Dobbyn A. J., Eckert F., Hampel C., Hetzer G., Lloyd A. W., McNicholas S. J., Meyer W., Mura M. E., Nicklass A., Palmieri P., Pitzer R., Schumann U., Stoll H., Stone A. J., Tarroni R., Thorsteinsson T.: *MOLPRO, A Package of Ab initio Programs*, version 2006.1 (2006), see http://www.molpro.net.
35. Werner H. J.: *Mol. Phys.* **1996**, *89*, 645.
36. Celani P., Werner H. J.: *J. Chem. Phys.* **2003**, *119*, 5044.
37. Frisch M. J., Trucks G. W., Schlegel H. B., Scuseria G. E., Robb M. A., Cheeseman J. R., Montgomery J. A., Jr., Vreven T., Kudin K. N., Burant J. C., Millam J. M., Iyengar S. S., Tomasi J., Barone V., Mennucci B., Cossi M., Scalmani G., Rega N., Petersson G. A., Nakatsuji H., Hada M., Ehara M., Toyota K., Fukuda R., Hasegawa J., Ishida M., Nakajima T., Honda Y., Kitao O., Nakai H., Klene M., Li X., Knox J. E., Hratchian H. P., Cross J. B., Bakken V., Adamo C., Jaramillo J., Gomperts R., Stratmann R. E., Yazyev O., Austin A. J., Cammi R., Pomelli C., Ochterski J. W., Ayala P. Y., Morokuma K., Voth G. A., Salvador P., Dannenberg J. J., Zakrzewski V. G., Dapprich S., Daniels A. D., Strain M. C., Farkas O., Malick D. K., Rabuck A. D., Raghavachari K., Foresman J. B., Ortiz J. V., Cui Q., Baboul A. G., Clifford S., Cioslowski J., Stefanov B. B., Liu G., Liashenko A., Piskorz P., Komaromi I., Martin R. L., Fox D. J., Keith T., Al-Laham M. A., Peng C. Y., Nanayakkara A., Challacombe M., Gill P. M. W., Johnson B., Chen W., Wong M. W., Gonzalez C., Pople J. A.: *Gaussian 03*, Revision C.02. Gaussian, Inc., Wallingford (CT) 2004.
38. Glendening E. D., Badenhoop J. K., Reed A. E., Carpenter J. E., Bohmann J. A., Morales C. M., Weinhold F.: *NBO 3.1*. Theoretical Chemistry Institute, University of Wisconsin, Madison 2001.
39. Hutter J., Luthi H. P., Diedrich F.: *J. Am. Chem. Soc.* **1994**, *116*, 750.
40. Botschwina P.: *J. Chem. Phys.* **1994**, *101*, 853.
41. Martin J. M. L., Taylor P. R.: *J. Phys. Chem.* **1996**, *100*, 6047.
42. Masso H., Veryazov V., Malmqvist P. A., Roos B. O., Senent M. L.: *J. Chem. Phys.* **2007**, *127*, 154318.
43. Jaszuński M., Dolgonos G., Dodziuk H.: *Theor. Chem. Acc.* **2002**, *108*, 240.
44. Pecul M., Helgaker T.: *Int. J. Mol. Sci.* **2003**, *4*, 143.
45. Allan M.: *J. Chem. Phys.* **1994**, *101*, 844.
46. Damiani D., Ferretti L., Gallinella E.: *Chem. Phys. Lett.* **1976**, *37*, 265.
47. Chiang J. F., Bauer S. H.: *J. Am. Chem. Soc.* **1970**, *92*, 1614.
48. Almennin A., Andersen B., Nyhus B. A.: *Acta Chem. Scand.* **1971**, *25*, 1217.

50. Wiberg K. B., Dailey W. P., Walker F. H., Waddell S. T., Crocker L. S., Newton M.: *J. Am. Chem. Soc.* **1985**, *107*, 7247.
51. Lazzeretti P., Malagoli M., Zanasi R., Della E. W., Lochert I. J., Giribet C. G., Deazua M. C. R., Contreras R. H.: *J. Chem. Soc., Faraday Trans.* **1995**, *91*, 4031.
52. Werner M., Stephenson D. S., Szeimies G.: *Liebigs Ann. Chem.* **1996**, 1705.
53. Jarret R. M., Cusumano L.: *Tetrahedron Lett.* **1990**, *31*, 171.
54. Della E. W., Cotsaris E., Hine P. T., Pigou P. E.: *Aust. J. Chem.* **1981**, *34*, 913.
55. Alber F., Szeimies G.: *Chem. Ber.* **1992**, *125*, 757.
56. Dawes R., Gough K. M.: *J. Chem. Phys.* **2004**, *121*, 1278.